Lateral response of caisson foundations :
A macroelement approach

N. Gerolymos, A. Zafeirakos & C. Souliotis
School of Civil Engineering, National Technical University, Athens

SUMMARY
The lateral undrained response of massive caisson foundations is investigated through a series of three-dimensional finite element analyses. The ultimate limit states are presented by failure envelopes in normalized form. The effects of embedment ratio and vertical load on the bearing capacity of the caisson is thoroughly examined. Closed-form expressions are proposed for (a) the yield surface in M-Q-N space, and (b) the lateral capacity under pure horizontal and moment loading. Finally, the validity of an associated flow rule to define the plastic deformation of the caisson at near failure conditions is parametrically identified. The results of the analysis could serve as a basis of a plasticity-based macro-element modelling.

Keywords: Caisson foundations, 3D finite element analysis, failure envelope, associated plastic flow rule, lateral capacity in undrained soil, Macro-element approach

1. INTRODUCTION

Although deep embedded caissons (ratio of embedment, D, to foundation width, B: *D/B* > 1) have been widely used to support major onshore and offshore structures, only a few methods have been devoted to the analysis of their monotonic and seismic response (e.g. Hutchinson et al. 2004, Silva and Manzari 2008, Gerolymos et al., 2009). In contrast, extensive literature exists on the bearing capacity of surface, shallow and embedded foundations (*D/B* ≤ 1) subjected to random loading. In these works, published by researchers involved mainly in offshore geotechnical engineering, the bearing capacity under combined vertical (*N*), horizontal (*Q*) and moment (*M*) loading is conveniently represented by a failure envelope in general three-dimensional N-Q-M load space (Roscoe and Schofield, 1957; Bransby and Randolph, 1998; Taiebat and Carter, 2000; Gourvenec and Randolph, 2003; Gourvenec, 2007, 2008; Randolph and Gourvenec, 2011).

At present, the most comprehensive "macro−element" models for soil−foundation interaction are based on work-hardening plasticity theory. In these models, the entire soil−foundation system is replaced by a single "element" located at the base of the superstructure aiming at reproducing the nonlinear soil-structure interaction effects taking place at the foundation level. The attractiveness of a macroelement approach is attributed to that: (a) computationally expensive 3-D nonlinear soil-structure interaction analyses can be avoided, and (b) foundation response at very small (nearly elastic) and at extremely large deformations are treated within a unified mathematical framework. Furthermore, macro−element modeling provide an effective means of communication between the geotechnical and structural engineers. If geotechnical engineers can express the load−displacement response of caisson foundations within this framework, then structural engineers can incorporate realistic foundation behaviour into their non-linear incremental structural analysis (Martin and Houlsby, 2000).

In this paper, the results from 3-D finite element analyses (with the use of code ABAQUS) are used for the calibration of a plasticity−based macro−element framework for static and cyclic response

analysis of caisson foundations in undrained cohesive soil. More specifically, the main objectives are: (a) to study the influence of embedment depth on caisson bearing capacity; (b) to identify the caisson failure envelope in N−Q−M space; (c) to check the validity of the associated plastic flow rule.
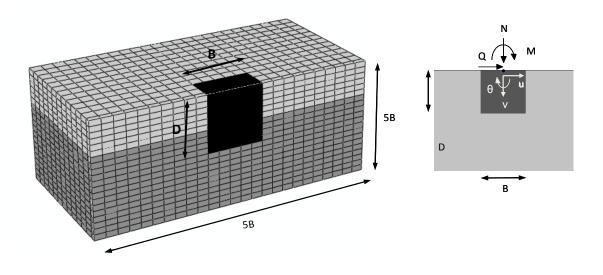

Figure 1. (a) The 3D Finite Element model used in the analysis, (b) sign convention for loads and displacements

2. PROBLEM DEFINITION AND ANALYSIS METHODOLOGY

2.1. Numerical Model

The studied problem is a caisson of width B and embedment depth D. Figure 1(a) shows a half-caisson cut through one of the orthogonal planes of symmetry. The size of the finite element mesh is *5B* x *5B* x *5B* in width, length and depth. Zero-displacement boundary conditions prevent the out of-plane displacements at the vertical sides of the model, while the base is fixed in all three coordinate directions. The effect of embedment (*D*) to width (*B*) ratio on the bearing capacity of the caisson, is parametrically investigated: D/B = 1, 2 and 3.

The foundation soil is an elastic-perfectly plastic material obeying to the von Mises yield criterion, with uniformly distributed undrained shear strength Su = 50 kPa, and stiffness ratio E / Su = 1000. The caisson is rigidly connected to the surrounding soil. In other words slippage in caisson−soil interface and separation of the caisson from the soil are not allowed. To ensure uniform stress distribution at the head of the caisson, the nodes of the associated elements are appropriately kinematically constrained.

2.2. Sign convention and nomenclature

The sign conventions for loads and displacements adopted in this paper, illustrated in Figure 1(b), obey a right-handed system and clockwise positive convention as proposed by Butterfield et al. (1997). The lateral capacities for pure loading are denoted by the subscript "u" (e.g. $Q = M = 0$ for $N = N_u$), whereas the maximum attained loads are subscripted with "max".

2.3. Load paths

The failure envelope is determined through a series of force−controlled analyses. Each analysis follows a single load path to failure in M-Q-N space. First, a vertical load is applied at the caisson head, monotonically increasing till a specified of χ is reached. Then, the vertical load is kept constant and the caisson head is subjected to a combined load of overturning moment and horizontal force
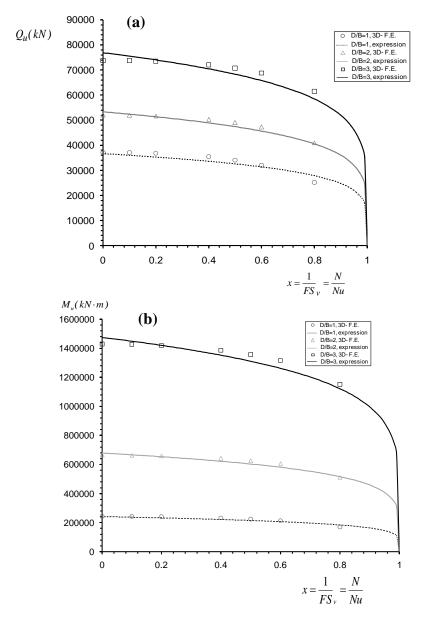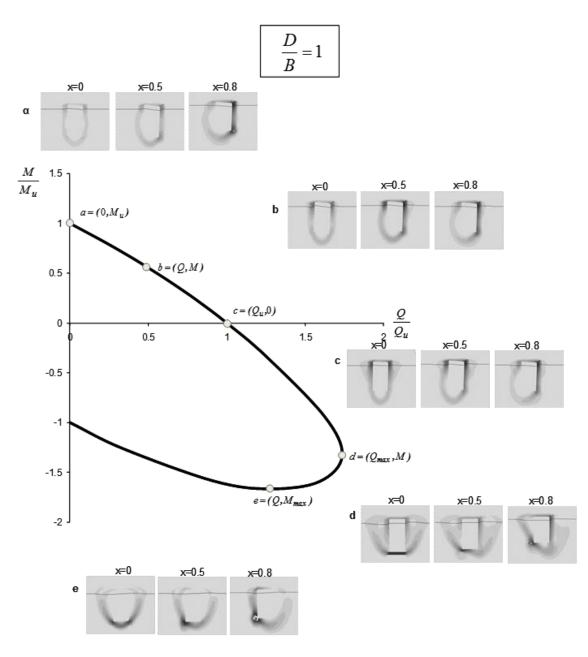
Figure 2. Comparison of the ultimate:
(a) horizontal force Q_u, and (b) overturning moment M_u, calculated with the FE and predicted by the simplified Eqs (1) and (2), for selected values of χ ($= 1 / FS_v$) and embedment ratio D/B

under a constant ratio M / Q (radial paths in the Q-M plane, Gouvernec 2004), till the complete failure of the caisson. Three different levels of vertical load are modeled, expressed through the parameter χ (denoting the inverse of the factor of safety: $1 / FSv = N / N_u$): 0 (zero vertical load), 0.5 and 0.8. The terminating points from each individual load path are used to determine a continuous failure envelope in Q-M plane.

Sideswipe analyses (introduced by Tan, 1990) are also performed to track the yield locus. The test method has been frequently adopted in several experimental (e.g. Martin and Houlsby, 2000) and numerical (e.g. Bransby and Randolph, 1997) studies. The procedure consists of two steps: (a) in the first step a vertical displacement is applied to the caisson until a specific vertical load is reached (corresponding to $\chi = 0$, 0.5 and 0.8); (b) in the second step a constant ratio of horizontal to rotational displacements is applied until failure of the caisson. Results will be presented in the sequel.

Figure 3. *Q–M* failure envelopes normalized by the respective lateral capacities at $\chi = 0$, Q_u, and M_u, respectively. Snapshots of the contours of plastic shear strain at failure are provided for characteristic points of the failure envelope and for three different values of $\chi = 0, 0.5, 0.8$. The embedment ratio of the caisson is D / B = 1

3. ANALYSIS RESULTS AND DISCUSSION

3.1. Ultimate capacity under pure loading

In general, embedment increases vertical, horizontal and moment capacity as failure mechanisms are forced deeper within the soil mass. Regarding the ultimate horizontal capacity Q_u of a caisson foundation, it is governed by a translational scoop mechanism due to coupling of the horizontal and moment degrees of freedom. As illustrated in Figure 2(a), Q_u depends on the magnitude of the applied vertical load (χ) and the embedment ratio (D/B). The following analytical expression is derived by fitting the numerical results:
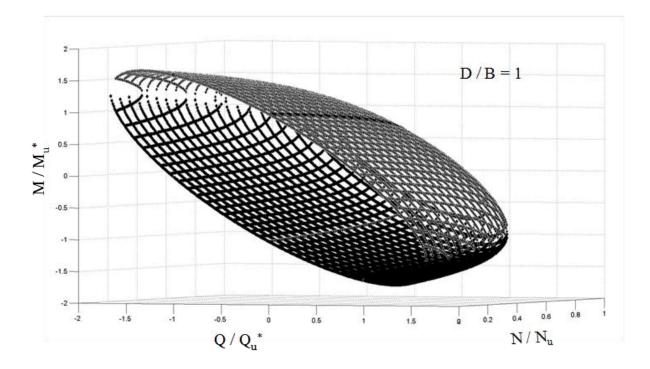
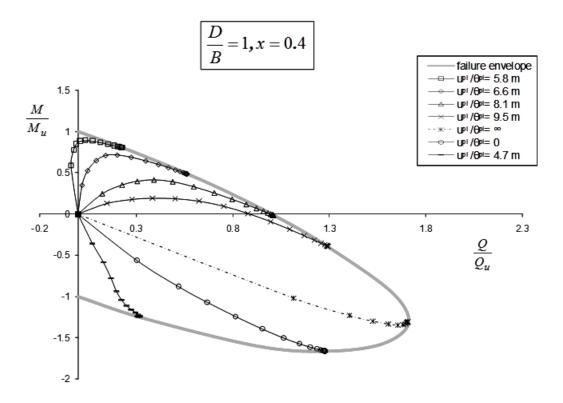**Figure 4**. Failure Envelope in 3D M-Q-N space from Equation 4. The caisson's embedment ratio is D / B = 1

Figure 5. Failure envelope from force−controlled analyses and swipe tests

$$Q_u = BDS_u(\frac{D}{B})^{-2.15}(1+\frac{D}{B})^{2.89}(1-x)^{0.17}$$

(1)

The ultimate moment capacity M_u of the caisson is governed by a scoop mechanism, with the scoop intersecting the edges of the base of the caisson and the center of rotation moving towards base level

with increasing embedment. The following simplified expression for M_u is derived (Figure 2b):

$$M_u = 0.46B^2 DS_u (\frac{D}{B})^{-1.49}(1+\frac{D}{B})^{3.39}(1-x)^{0.17}$$

(2)

3.2. Failure envelopes

A series of FE calculations are carried out to deduce the failure envelopes in *M-Q* space, under constant vertical load: $\chi = 0, 0.1, 0.2, 0.4, 0.5, 0.6$ and 0.8. Three different embedment ratios are examined: *D / B* = 1, 2 and 3. Figure 3 depicts a representative envelope calculated for *D/B* = 1 and $\chi = 0, 0.5$ and 0.8, along with the associated contours of plastic shear deformations. The applied horizontal force, *Q*, and overturning moment, *M*, are normalized with the respective ultimate capacities. For embedment ratios *D/B* $\geq$ 1 this normalization leads to identical shapes irrespectively of the value of χ. The following observations are worthy of note:

- In all envelopes the maximum moment M_{max} is sustained with a positive horizontal load, where the maximum horizontal load Q_{max} requires negative moment loading.
- As the vertical load (χ) increases, the symmetry in the failure mechanisms is lost and a clear accumulation of plastic deformations is observed towards the direction of the predominant loading.

The points along the surface correspond to:

(a) pure moment loading, M_u, with a rotational "scoop" mechanism prevailing at failure
(b) combined positive *M-Q* loading, resulting again in a narrow forward "scoop" mechanism
(c) pure horizontal loading, Q_u, which results in a deeper forward "scoop"
(d) maximum horizontal loading, Q_{max}, for which the mobilization of additional active and passive side-wall resistances result in a sliding mechanism along the base of the caisson
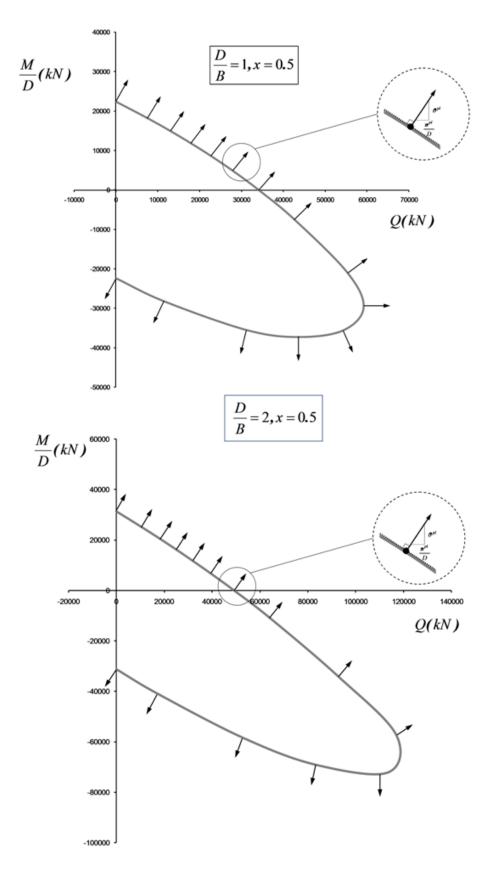(e) maximum moment loading, M_{max}, where a "scoop-slide" mechanism prevails

Relevant studies on embedded foundations suggested that the shape of the yield function can be described by an oblique parabola in *M-Q* space. In the present work, the following expression was found to better match the numerical results:

$$f = (\frac{Q}{Q_u})^2 + (\frac{M}{M_u})^2 + n_3(\frac{Q}{Q_u})(\frac{M}{M_u}) - 1 = 0$$

(3)

where n_3 is a parameter controlling the shape of the surface. Eq.(3) can be rewritten in a more suitable form by extracting the term N / N$_u$ from the lateral capacities Q$_u$ and M$_u$:

$$f = (1 - \frac{N}{N_u})^{-0.34}\left[(\frac{Q}{Q_u^*})^2 + (\frac{M}{M_u^*})^2 + n_3(\frac{Q}{Q_u^*})(\frac{M}{M_u^*})\right] - 1 = 0$$

(4)

In which, $N / N_u = \chi$, $Q_u^* = Q_u$ at $\chi = 0$, and $M_u^* = M_u$ at $\chi = 0$. The regression analysis resulted in the following expression for n_3 :

Figure 6. Yield Surface and associated plastic flow rule, calculated from the FE analysis for embedment ratios $D / B = 1$ and 2, and for $\chi = 0.5$ ($FS_v = 2$)

$$n_3 = 1.84 - 0.21(\frac{D}{B})^{-1.98}$$

<div align="right">(5)</div>

The 3-Dimensional failure envelope described by Eq (4) is visualized in Figure 4, for D / B = 1. The corresponding cross section at χ = 0.4 (FS$_v$ = 2.4) is depicted in Figure 5, and compared with that from the swipe tests. The swipe tests are performed by prescribing a fixed ratio of horizontal displacement to rotation (u^{pl} / θ^{pl}) at constant χ, until failure is finally reached. Observe the striking agreement between the points along the failure calculated from both methods, providing strong support for the validity of the methodology followed in this paper. It is interesting to note that, at Q_{max} (point (d) in Figure 3), the ratio $u^{pl} / \theta^{pl} \to \infty$, whereas, at M_{max} (point (e) in Figure 3) , the ratio $u^{pl} / \theta^{pl} \to 0$ in point.

3.3. Flow rule

In addition to assessing the shape of the failure envelope, the force−controlled analyses are used to estimate the displacement increments at yield ($\dot{u}_p, \dot{\theta}_p$). These provide guidance on a suitable flow rule for use in conjunction with the M-Q-N yield surface. Figure 6 plots the vectors of the relative magnitude displacements ($\dot{u}_p, \dot{\theta}_p / D$) on yield surfaces in $Q−M/D$ space accordingly, for χ = 0.5 and embedment ratios D/B = 1 and 2. Notice that the incremental displacement vectors are all approximately normal to the rotated ellipses, indicating that an associated flow rule is applicable in the $Q−M/D$ plane. This normality condition was satisfied in every examined case of χ and D/B.

4. CONCLUSIONS

3-dimensional finite element analyses of square caisson foundations embedded in undrained soil and subjected to combined M-Q-N loading were carried out, emphasizing the effects of embedment depth and vertical factor of safety on the failure modes of the caisson. The results were utilized in the establishment of analytical expressions for the failure envelope (yield surface in M-Q-N loading space) and plastic flow rule, that could serve as a basis for a macro-element approach.

REFERENCES

ABAQUS 6.1. (2001). Standard user's manual. Rhode Island: Hibbit, Karlsson and Sorensen.

Bransby, M. F., Randolph, M.F. (1997). Shallow foundations subject to combined loadings. *9th International Conference of the International Association for Computer Methods and Advances in Geomec*, **3**, 1947~1952.

Bransby, M. F., Randolph, M. F. (1998). Combined loading of skirted foundations, *Geotechnique*, **48**(**5**): 637~655.

Butterfield, R., Houlsby, G. T., Gottardi, G. (1997). Standardized sign conventions and notation for generally loaded foundations, *Geotechnique*, **47**(**4**): 1051~1054.

Gerolymos, N., Drosos, V., Gazetas, G. (2009). Seismic response of single-column bent on pile: evidence of beneficial role of pile and soil inelasticity. *Bull Earthq Eng* **7**(**2**): 547–573 Special Issue: Earthquake Protection of Bridges.

Gourvenec, S. (2004). Bearing capacity under combined loading - a study of the effect of shear strength heterogeneity. *9th Australian and New Zealand Conference on Geomechanics*, Auckland, New Zealand, pp. 527-533.

Gourvenec, S. (2007). Failure envelopes for offshore shallow foundation under general loading, *Geotechnique*, **57**(**9**): 715~728.

Gourvenec, S. (2008). Effect of embedment on the undrained capacity of shallow foundations under general loading, *Geotechnique*, **58**(**3**): 177~185.

Gourvenec, S. and Randolph, M. F., (2003). Effect of strength non-homogeneity on the shape and failure envelopes for combined loading of strip and circular foundations on clay, *Geotechnique*, **53**(**6**): 575~586.

Hutchinson, T.C., Chai, Y. H., Boulanger, R.W., Idriss, I.M. (2004). Inelastic Seismic Response of Extended Pile-Shaft-Supported Bridge Structures. *Earthquake Spectra*, **20**(**4**): 1057-1080.

Martin, C. M., Houlsby, G. T. (2000). Combined loading of spudcan foundations on clay: laboratory tests, *Geotechnique*, **50**(**4**): 325~338.

Randolph, M.F., Gourvenec, S. (2011). Offshore Geotechnical Engineering. Spon Press, UK.

Roscoe, K. H., Schofield, A. N. (1957). The stability of short pier foundations in sand, discussion, *British Welding Journal*, January, 12~18.

Silva, P.F., Manzari, M.T. (2008). Nonlinear Pushover Analysis of Bridge Columns Supported on Full-Moment Connection CISS Piles on Clays. *Earthquake Spectra*, **24** (**3**), pp. 751-774.

Taiebat, H. A., Carter, J. P. (2000). Numerical studies of the bearing capacity of shallow foundations on cohesive soil subjected to combined loading. *Geotechnique*, **50** (**4**), pp. 409–418.

Tan, F. S. (1990). Centrifuge and Theoretical Modelling of Conical Footings on Sand. Ph. D. thesis, University of Cambridge.